Surface & Coatings Technology 320 (2017) 91–96

Contents lists available at ScienceDirect

Surface & Coatings Technology

journal homepage: www.elsevier.com/locate/surfcoat

Cross- and in-plane thermal conductivity of AlN thin films measured using differential 3-omega method

Manuel Bogner [a,b,*], Günther Benstetter [a], Yong Qing Fu [b,**]

[a] Deggendorf Institute of Technology, Edlmairstr. 6 + 8, 94469 Deggendorf, Germany
[b] Faculty of Engineering and Environment, Northumbria University, Newcastle upon Tyne NE1 8ST, UK

ARTICLE INFO

Article history:
Received 30 August 2016
Revised 23 January 2017
Accepted in revised form 25 January 2017
Available online 27 January 2017

Keywords:
Aluminum nitride
Thermal conductivity
Three omega method
Thermal management
Thin films

ABSTRACT

Thickness dependency and interfacial structure effects on thermal properties of AlN thin films were systematically investigated by characterizing cross-plane and in-plane thermal conductivities, crystal structures, chemical compositions, surface morphologies and interfacial structures using an extended differential 3ω method, X-ray diffraction (XRD) analysis, X-ray photoelectron spectroscopy, atomic force microscopy (AFM) and transmission electron microscopy. AlN thin films with various thicknesses from 100 to 1000 nm were deposited on p-type doped silicon substrates using a radio frequency reactive magnetron sputtering process. Results revealed that both the cross- and in-plane thermal conductivities of the AlN thin films were significantly smaller than those of the AlN in a bulk form. The thermal conductivities of the AlN thin films were strongly dependent on the film thickness, in both the cross- and in-plane directions. Both the XRD and AFM results indicated that the grain size significantly affected the thermal conductivity of the films due to the scattering effects from the grain boundary.

1. Introduction

Aluminum nitride (AlN) thin films have been widely used in surface acoustic wave devices [1,2], light emitting diodes [3], and micro-electro-mechanical systems because of their outstanding properties, such as high piezoelectric coupling factor, excellent dielectric properties, wide band-gap, and high thermal conductivity. With the decrease of structural dimensions and simultaneous increase of power density for many microelectronic devices, it is urgent to use high thermally conductive and insulating thin films or coatings, such as AlN, to replace some traditional dielectric layers such as SiO_2. Single crystalline AlN is one of the promising candidates for effective heat conductors in microelectronic devices due to its high thermal conductivity (320 Wm^{-1} K^{-1}) at room temperature [4], which makes it an ideal material to solve the thermal management problem. The bulk thermal conductivity of the AlN is significantly higher than those of standard dielectric materials such as silicon dioxide (SiO_2) and silicon nitride (Si_3N_4) [5,6]. However, thermal conductivities of thin film and coating materials could be substantially different from those of their bulk counterparts [5,7–11], which are generally attributed to two main reasons. Firstly, compared to the bulk crystalline materials, many thin films prepared using deposition technologies have many impurities, dislocations, and grain boundaries, all of which tend to reduce the thermal conductivity of the films [6,8,11]. Secondly, even though the film with less defects can be prepared, it is still expected to have reduced thermal conductivity due to grain boundary scattering and phonon leakage in the thin film materials. These two effects affect cross-plane and in-plane heat transport differently, so that the thermal conductivities of the thin films are generally anisotropic in these two directions, even though their bulk counterparts have the isotropic properties. Therefore, precise measurement of the cross-plane (λ_x) and in-plane (λ_z) thermal conductivities of polycrystalline thin films such as AlN is critical for designing or analysing the microelectronic devices. Besides crystalline quality and compositions of AlN thin films, the interfacial structure between the film and substrate is another important factor in determining the thermal conductivity of the whole device, and is critical for the reliability and efficiency of the AlN based devices operated at high powers [11]. To ensure the best thermal performance of AlN thin films and coatings, it is necessary to systematically study the relationships among the process parameters, microstructures such as crystallinity and interfacial properties and thermal conductivity of the films.

This work reports a new approach to measure both cross- and in-plane thermal conductivities λ of thin films prepared on silicon substrates using magnetron reactive sputtering, in order to characterize the thickness dependency of the film's thermal conductivity. Experimental work and theoretical analysis have been conducted to understand the effects of crystallinity, grain sizes, and interfacial structures

* Correspondence to: M. Bogner, Deggendorf Institute of Technology, Edlmairstr. 6 + 8, 94469 Deggendorf, Germany.
** Corresponding author.
E-mail addresses: manuel.bogner@th-deg.de (M. Bogner), richard.fu@northumbria.ac.uk (Y.Q. Fu).

http://dx.doi.org/10.1016/j.surfcoat.2017.01.100

of the AlN films on their thermal conductivities. It is for the first time that both the cross- and in-plane thermal conductivities of the thin films were measured using an improved differential 3ω method. In contrast to the commonly used thermal conductivity measurement methods, such as laser ablation [10], AC calorimetric [12] method or photothermal reflectance [5], the improved differential 3ω method is insensitive to errors from black-body radiation because the effective thickness of the sample is extremely small [13]. Therefore, higher accuracy and better reproducibility of the film's thermal conductivity data can be obtained.

2. Experimental

In this work the cross- and in-plane thermal conductivities of the AlN thin films were determined using the differential 3ω method, which was originally developed by Cahill [13]. The 3ω measurement technique was evolved from the conventional hot-wire techniques and is currently widely used to measure the cross-plane thermal conductivity of dielectric thin films [9,14]. As shown in Fig. 1, a thin metal strip, with a width of *2b* and a resistance R_h, is deposited on top of the thin film sample for simultaneous operations as both a heater and thermometer. An alternating current with an angular modulation frequency ω is driven through the metal strip causing Joule heating and induces a temperature oscillation $\Delta T(\omega)$ at a frequency of 2ω. This results in a voltage oscillation $\Delta V(\omega)$ along the heating resistor with a third harmonic which depends on the temperature oscillation of the heater. The temperature and voltage oscillations are the key parameters of the differential 3ω method. Using the differential 3ω method, thermal conductivity of a thin film can be obtained by comparing the temperature oscillation in a film-on-substrate structure with the corresponding value of the substrate. The temperature variation of the film-on-substrate structure can be experimentally measured by detecting the voltage oscillation across the metal heater, which is proportional to the oscillating resistance value. The substrate temperature oscillation can be determined by [14]:

$$\Delta T = \frac{P}{\pi l \lambda_s}\left(\frac{1}{2}\ln\frac{4D}{b^2} + \ln 2 - 0.5772 - \frac{1}{2}\ln(2\omega) - \frac{i\pi}{4}\right) \quad (1)$$

where λ_s is the thermal conductivity of the substrate, *D* the thermal diffusivity of the substrate, *P* the power supplied to the metal strip, *l* the length of the metal strip and *i* the imaginary unit, respectively.

If the thermal conductivity λ_f of the thin film is much smaller than that of the substrate material and also the width *2b* of the metal strip is much larger than the thickness d_f of the investigated film, the temperature shift induced by the thin film ΔT_f is given by [9]:

$$\Delta T_f = \frac{P\, d_f}{l \lambda_f 2b} \quad (2)$$

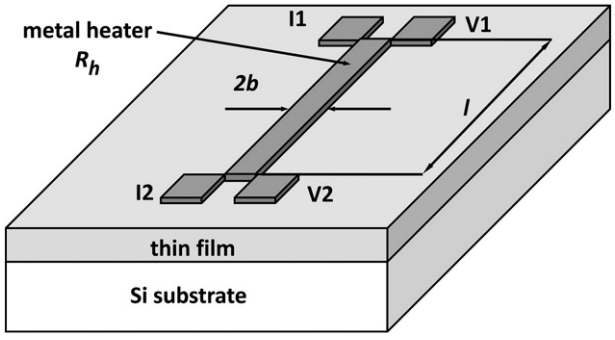

Fig. 1. Schematic layout of the four-pad test structure used to determine the cross-plane thermal conductivity of a thin film by the differential 3ω method. A metal strip serves as both the heater and the thermometer. The four pads are the connections for current leads (I1, I2) and voltage leads (V1, V2). *l* is the distance between the current leads and *2b* is the strip width.

Measurements of the in-plane thermal conductivity are less common than those of the cross-plane direction, while the methods used are more diverse. In-plane measurements can be divided into those for the suspended and supported films. In general, methods for the suspended films are only sensitive for the in-plane thermal conductivity and cannot properly detect the heat flow in the cross-plane direction [15]. Furthermore, the microfabrication to obtain a suspended thin film is sometimes a serious challenge. Therefore, the suspended film method is not widely used for thermal measurements in the cross-plane direction of thin films.

In this study, we used our extended variable line width 3ω method for the supported films because of two main reasons. Firstly, we want to focus on simultaneously measuring the cross- and in-plane thermal conductivities of the thin films without changing the sample during the measurement, which allows a precise comparison of cross- and in-plane conductivities. Secondly, compared to the other methods, the variable line width technique works better for thin films with a small to moderate λ_z value [15]. The measurement principle for the in-plane measurement is the same as that for the cross-plane 3ω measurement. As for the cross-plane technique, the surface of the thin film is heated over a finite region by a metal strip, and the lateral spreading of the heat inside the film modifies the temperature distribution, which is different from the one for a strictly one-dimensional case. The lateral heat spreading is governed by the thickness and thermal conductivity of the film and also by the dimensions of the metal heater. By comparing the temperature rises in the metal heaters with different widths, the cross- and in- plane thermal conductivities can be obtained.

The cross-plane 3ω method requires the usages of wide metal heaters such that the heat flow is perfectly one-dimensional in the *z* direction, making the measurement sensitive only to the film's cross-plane thermal conductivity λ_z. However, it is also possible to exploit the opposite extreme situation in which a large in-plane heat can be generated and then spread in order to determine the value of λ_x [15,16]. The narrow-heater regime can be defined as $(b/d_f)(\lambda_z/\lambda_x)^{1/2}$ of about 0.1 or less. In this case, the thermal resistance of the film R_f is sensitive to both λ_x and λ_z, so it is a standard practice to prepare a second heater with a much larger width to independently obtain the in-plane thermal conductivity λ_z of the thin film. A better accuracy could be achieved by measuring a series of multiple heater widths and fitting the observed R_f data using the following equation [16]:

$$\frac{R_f}{d_f/2\lambda_z bl} = \frac{2}{\pi}\left(\frac{b}{d_f}\right)\left(\frac{\lambda_z}{\lambda_x}\right)^{1/2}\int_0^\infty u^{-3}\sin^2(u)\,\tanh\left[u\left(\frac{b}{d_f}\right)\left(\frac{\lambda_z}{\lambda_x}\right)^{1/2}\right]du \quad (3)$$

In this work, we improved the sensitivity and accuracy of the novel in-plane measurement by measuring a series of multiple heaters with different widths *2b* and constant length *l*. Therefore, we deposited four metal heaters on top of the AlN thin film sample. The heater width was varied between 1.5 and 20 μm in order to be able to obtain both the cross- and in-plane thermal conductivities of the AlN thin films with a better accuracy. The improved metal heater setup for the thermal conductivity measurement is shown in Fig. 2. Additional details about the differential 3ω technique can be found from various references [9,14,15] and are therefore not discussed in detail here. Furthermore, our new 3ω method for simultaneously measuring the cross- and in-plane thermal conductivity can be applied to study very thin and unconventional coating materials.

The AlN thin films were deposited onto p-type doped silicon (100) substrates using a radio frequency reactive magnetron sputtering process with an RF power of 5 kW. The ambient pressure and temperature

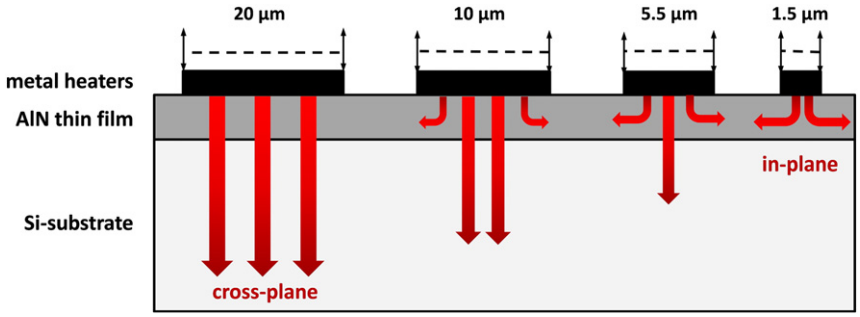

Fig. 2. Cross-sectional schematic of the improved microstructure used for measuring both the cross- and the in-plane thermal conductivities in the same AlN thin film. The metal strips of line width *2b* varying between 1.5 and 20 μm are deposited on the same thin film sample. When the metal strip width is much larger than the thin film thickness, the thermal conduction is nearly one dimensional in the direction normal to the film, and the cross-plane conductivity has a dominant influence on the temperature rise. On the other side, the sensitivity of the measurement to the in-plane conductivity increases with decreasing values of the ratio of the strip width to the film thickness.

in the deposition chamber were controlled to be 9.5 mTorr and 25 °C, respectively. An aluminum target (99.9995% purity) of 5 in. (12.7 cm) in diameter was utilized for deposition of AlN film with a gas mixture of N_2 (50 sccm) and Ar (10 sccm). The purity of nitrogen (N_2) and argon (Ar) gases was 99.995%. Before the AlN deposition, the substrates were ultrasonically cleaned in acetone, ethanol, and de-ionized water sequentially. Then, they were etched in 10% hydrofluoric acid (HF) solution to remove the native oxide layers on their surfaces. The substrates were transferred into a high vacuum chamber right after being dried using N_2. The thicknesses of the deposited AlN films were between 100 and 1000 nm in order to characterize the thickness dependency of the film thermal conductivity. After the deposition process, the film thickness was measured using a surface profilometer (Tencor P-20H). The metal heaters were deposited onto the thin film sample using a lift-off process. Gold (Au) was used as the heater material because of its high temperature stability and high temperature coefficient of resistance. The lithography mask used here was designed to yield gold heaters of line widths varied between 1.5 and 20 μm and a length of 9 mm on the same die as shown in Fig. 2. Measured data obtained from the metal heaters with varied widths enable one to extract both the cross- and in-plane thermal conductivities of the same AlN thin film sample. The Au-heater was about 500 nm in thickness. Between the AlN thin film and the Au strip, a 60 nm thin platinum titanium layer was pre-deposited to improve the adhesion strength.

The main challenge of the experimental setup is the reliable extraction of the 3ω voltage signals from the voltage oscillations of the thin film sample, since the amplitude of the 1ω voltage is typically 100 to 1000 times larger than that of the 3ω voltage [9]. Therefore, an appropriate electrical circuit, consisting of a differential lock-in amplifier and a bridge circuit, is needed. Fig. 3 shows a schematic diagram of the experimental setup used to extract the 3ω component of the voltage along the metal heater. An internal signal generator of the digital lock-in amplifier (Anfatec Instruments eLockIn204/2) produces the alternating heating current. The generated heating current contains a low harmonic distortion, because any third harmonic content in the signal generator can induce interfering signals during the thermal conductivity measurement. Due to the finite dynamic reserve of the lock-in amplifier (24 dB), the suppression of the 1ω voltage from the 3ω signal is accomplished by a bridge circuit balanced by adjusting the series reference resistance R_{ref}. The reference resistance R_{ref} needs a low temperature coefficient of resistance and also a low thermal resistance to the environment to minimize any spurious 3ω artifacts, which could influence the measurement of the third harmonic voltage. To properly detect the 1ω and 3ω voltage signals, a differential lock-in amplifier with a bandwidth of 0.1 Hz up to 2 MHz was used. In order to reduce radiation and convection losses, the measurement was performed inside a vacuum chamber with a pressure less than 3.1 Pa.

The crystal structures of the AlN films were studied by X-ray diffraction (XRD). The surface morphologies and surface nodule sizes of the AlN films were investigated by a Bruker Dimension 3100 atomic force microscope (AFM). The AlN/Si interface region, which is considered as an important factor for thermal performance, was examined by cross-sectional transmission electron microscopy (TEM). The structures of the AlN/Si interface were investigated by Tecnai G2 F20 TEM with an accelerating voltage of 200 kV. Additionally, the grain sizes of AlN films were investigated by the TEM and then compared with those estimated by the Scherrer equation from the XRD analysis. As a semi-quantitative method, X-ray photoelectron spectroscopy (XPS) was also employed to analyze the chemical compositions of the deposited AlN films.

3. Results and discussion

In this study, the differential 3ω technique was used to analyze the thickness dependency of the cross- and in-plane thermal conductivities

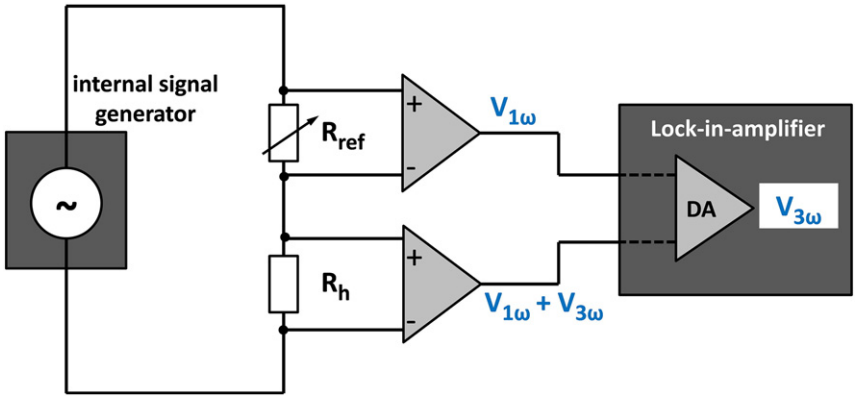

Fig. 3. Schematic circuit diagram used to extract the 3ω voltage component from the voltage signal across the metal strip deposited on the sample.

of the AlN thin films. Firstly, the thermal conductivity λ_s of the Si substrate must be determined in order to set the ΔT reference for the differential 3ω method. The thermal conductivity of the Si substrate determined by Eq. (1) is 141 $Wm^{-1} K^{-1}$, which is approximately 5% smaller than the literature value of pure Si 148 $Wm^{-1} K^{-1}$ [9,13,14] and about 6% higher than the literature value of p-doped Si 134 $Wm^{-1} K^{-1}$ [17]. It is evident that this discrepancy is mainly due to the impurity scattering by the doped boron in the silicon substrate [11]. The random error of the measurement for a given AlN or Si sample, based on ten or more measurements, was found to be better than 3% in all cases.

Table 1 lists the experimental results of the cross- and in-plane thermal conductivities of the AlN films as a function of the film thickness. The thermal conductivity values of the AlN film samples with thicknesses varied from 100 to 1000 nm are between 3.2 and 14.9 $Wm^{-1} K^{-1}$ for the cross-plane cases and between 10.2 and 18.6 $Wm^{-1} K^{-1}$ for the in-plane cases. Table 1 indicates that the in-plane thermal conductivities of the AlN thin films are significantly higher than the cross-plane ones. The main reason to explain this result is that along the in-plane direction, phonons traveling along directions parallel to the interface are not disturbed, whereas those along the cross-plane direction have a limited mean free path due to the film thickness and boundary scattering at the interfacial structures between the thin film and substrate [15]. The experimental values for both the cross- and in-plane directions are substantially lower than those of the corresponding bulk material which is around 320 $Wm^{-1} K^{-1}$ [4]. Furthermore, the film thermal conductivity values of both the cross- and in-plane directions increase with the film thickness, but the increase rate of the cross-plane conductivity gradually decreases with increasing the film thickness as shown in Fig. 4.

In order to correlate the measured thermal conductivity values with the microstructures of the film, XRD patterns of AlN (220) peaks have been obtained and the results are summarized in Fig. 5. XRD analysis reveals that the AlN thin films are of crystalline structure regardless of the thickness. It was reported that the grain size significantly affected the thermal conductivity due to the grain boundary scattering effect and larger grain size enhanced the thermal conductivity because of the longer phonon mean free path [6,8]. According to this finding, the results of the XRD analysis in this study were used to determine the grain sizes of the AlN thin films. The average grain size of the thin film can be calculated using the Scherrer equation:

$$D_P = \frac{K \cdot \gamma}{\beta \cdot \cos\theta} \tag{4}$$

where K is the dimensionless shape factor, γ the X-ray wavelength, β the line broadening at half the maximum intensity (FWHM) in radians, θ the Bragg angle, respectively. Table 1 lists the determined average grain size values as a function of the AlN film thickness. The values for the grain size are between 11 and 119 nm for the AlN films with thicknesses varied from 100 to 1000 nm. The average grain size values increase with the film thickness. To verify the grain size estimated by the Scherrer equation, the average grain size of the 300 nm AlN film was investigated using the TEM, and the obtained grain size value of the 300 nm AlN film is about 26 nm. This is nearly the same value which was obtained using the Scherrer equation.

Table 1
Experimental results of the cross- and in-plane thermal conductivity of AlN thin films by the differential 3ω method, the average grain size of the investigated AlN thin films determined by the results of the XRD measurements by Eq. (4) and the calculated thermal conductivity of the polycrystalline AlN films with different grain sizes by Eq. (5).

Film thickness d_f [nm]	Thermal conductivity value λ_f [$Wm^{-1} K^{-1}$]		Average grain size value D_P [nm]	Thermal conductivity values calculated by Slacks model λ_p [$Wm^{-1} K^{-1}$]
	Cross-plane λ_z	In-plane λ_x		
100	3.2	10.2	11	16
300	8.5	12.5	28	37
500	11.0	13.9	45	55
700	13.2	16.4	66	75
1000	14.9	18.6	119	114

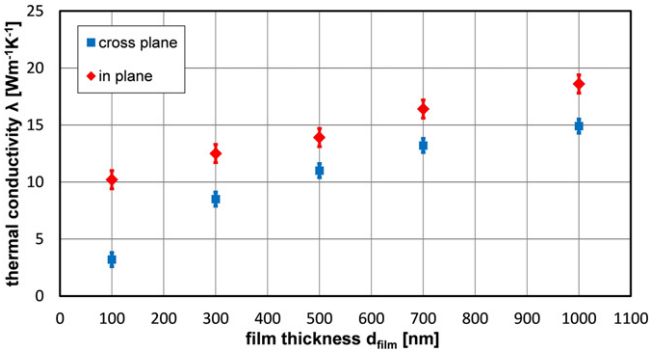

Fig. 4. Cross- and in-plane thermal conductivity of AlN thin films as a function of film thickness. The squares represent the experimental data of the in-plane conductivity and the diamonds the cross-plane conductivity data obtained in this study by an advanced differential 3ω method.

To support the grain size estimation by the Scherrer equation and TEM analysis, the surface morphologies and average surface nodule sizes of the AlN films were investigated by AFM. Fig. 6 presents the AFM images showing the surface morphologies of the 300, 500, and 700 nm AlN films with smooth surfaces and uniform grains. With the decrease of film thickness, no obvious changes in surface roughness were observed. The average surface nodule sizes for AlN films with film thicknesses of 300, 500, and 700 nm are 31, 59, and 77 nm, respectively, suggesting that the surface nodule size decreases slightly with decreasing film thickness. Therefore, the surface nodule sizes for the AlN thin films measured by the AFM support the grain size results obtained by the Scherrer model. According to these results, it can be derived that the increased thermal conductivity of the AlN thin films for a thicker film is primarily due to the increase in the grain size. In addition, the reduction of the thermal conductivity values in comparison to the bulk values can be attributed to the shorter mean free path of the phonons.

Slack et al. [6] reported that the grain size significantly affected the thermal conductivity due to the grain boundary scattering, because a smaller grain size could decrease the thermal conductivity of the film due to the shorter phonon mean free path. Furthermore, Choi et al. [11] and Pan et al. [8] analyzed the XRD patterns of the AlN thin films in order to correlate the measured thermal conductivity with the microstructure of the films. They found that according to the XRD results, the increased thermal conductivity of thicker AlN thin films was primarily due to the increase in the grain size [6,8,11]. The experimental results obtained from our AlN thin films support this observation.

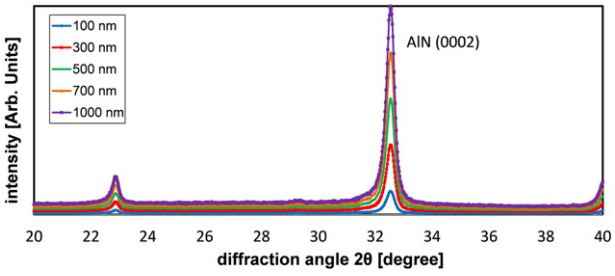

Fig. 5. The XRD 2θ scan patterns (0002) of AlN thin films deposited on Si substrates. The thickness of the thin films varied between 100 and 1000 nm.

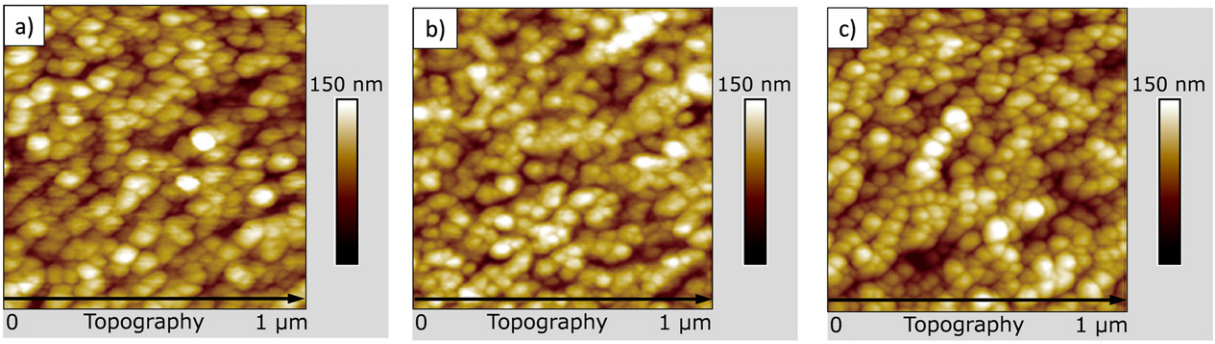

Fig. 6. The AFM images of AlN films deposited on Si substrates with film thicknesses of a) 300 nm, b) 500 nm, and c) 700 nm to study the surface morphology and average surface nodule size.

Slack et al. [6] proposed a model for the grain-size dependence of the cross-plane thermal conductivity of the polycrystalline AlN. In this model, the thermal conductivity λ of the polycrystalline AlN with an average grain size of D_p can be determined by:

$$\lambda_p^{-1} = \left(D_p \cdot v \cdot \frac{C}{3}\right)^{-1} + \lambda_{pp}^{-1} \quad (5)$$

where v is the average sound velocity (6.98×10^3 m·s^{-1}), C is the specific heat capacity per volume, and λ_{pp} is the thermal conductivity of the AlN single crystal. Using the average grain sizes obtained from the XRD results, the thermal conductivity of the polycrystalline AlN films with the grain sizes between 11 and 119 nm can be calculated using the Slack's model. The results are listed in Table 1. The calculated values suggest that the difference in the grain sizes for the different film thicknesses changes the thermal conductivity of the AlN film. However, the calculated thermal conductivity λ values are higher than the experimental data of our AlN films. This is reasonable since only the grain boundary scattering effect has been taken into account in the Slack's model. In other words, the obtained data imply that there are other mechanisms besides the grain boundary scattering which significantly affect the thermal conductivity in our study.

XPS was employed to analyze the chemical compositions of the deposited AlN films. Table 2 shows the obtained atomic ratios of Al, N, and O elements of each AlN film. As a common impurity of sputtered AlN films, the oxygen impurity was observed in all the AlN films in this study. The ratios of oxygen content in films, which were fluctuant with a poor dependence on film thickness, are in the range between 9% and 11%. Oxygen, which is a part of air, is hard to be completely removed from the vacuum chamber. During the growth of AlN films, the residual oxygen atoms in the chamber can easily form Frenkel and or Schottky-type defects in the AlN lattice. It should be noted that XPS is a semi-quantitative characterization method, thus the atomic ratios gained from XPS data might not be the exact concentrations of oxygen defects in our AlN films (generally over-estimated).

It is noticed that the calculated effective thermal conductivity by Eq. (5) Slack's model [6] is higher than the experimental data of our AlN films. This difference may be caused by the phonon scattering induced by oxygen defects as supported by XPS results, and/or other mechanisms such as a lattice mismatch at the AlN/Si interface. For thin films, the interfacial region near the substrate generally has distorted or amorphous microstructures because of the lattice mismatch and the existence of surface defects. Furthermore, the oxygen content, which causes the phonon scattering of defects and leads to a reduction in thermal conductivity, shows a weak correlation with the film thickness, as indicated by the XPS data. In other words, the improvement of interface structure may be a main reason for the enhancement of thermal conductivity of the investigated AlN films in our study.

In Fig. 4, there is a significant decrease in the cross-plane thermal conductivity at around 300 nm, which is due to a lattice mismatch at the AlN/Si interface. For thin films, the interfacial region near the substrate generally has distorted or amorphous microstructures because of the lattice mismatch and the existence of surface defects [8,11]. Consequently, considering the differences in the lattice constants of the AlN (3.2 Å) and Si (5.3 Å), it is expected that the AlN thin film might have a graded interfacial layers, thus the thermal conductivity of the 300 nm thick film in Fig. 4 could be an average values of this graded layer structure.

To support this theoretical statement, the structures of the AlN/Si interface were further investigated by TEM. Fig. 7 shows the typical TEM bright-field image taken at the AlN/Si interface of the 300 nm AlN film. A thin amorphous AlN layer with a thickness of about 5 nm can be observed at the interface of the film. However, the texture quality

Table 2
The atomic ratio of aluminum, nitrogen, and oxygen in the deposited AlN films obtained by XPS measurements.

Film thickness d_f [nm]	Aluminum [%]	Nitrogen [%]	Oxygen [%]
100	58.1	32.1	9.8
300	57.2	32.3	10.5
500	58.4	31.9	9.7
700	56.9	33.1	10.0
1000	55.9	34.6	9.5

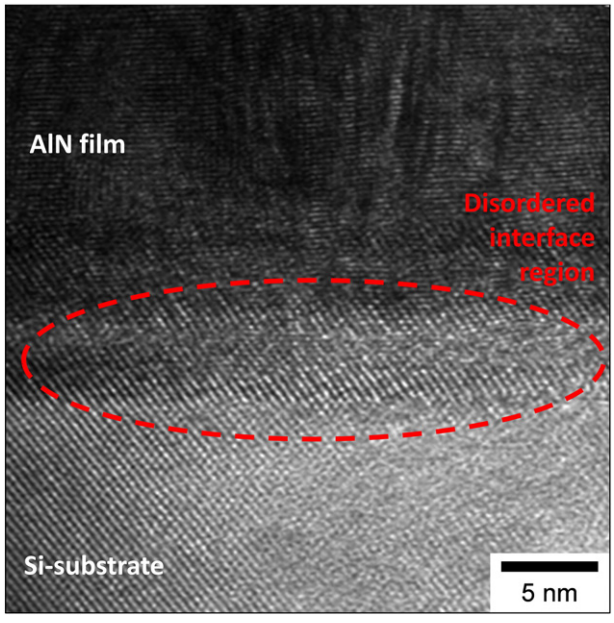

Fig. 7. The cross-sectional TEM image of the 300 nm thin AlN film deposited on Si substrate in order to investigate the structure of the AlN/Si interface.

in the vicinity of the amorphous layer is much better than that of the interface region. The evolution of amorphous and disordered AlN/Si interfacial region in the AlN thin film reveals that the interface scattering is another important factor, which influences the thermal conductivity of the thin films, especially in the cross-plane direction.

This amorphous interfacial layer has also been observed by other groups in sputtered AlN films on Si substrates [8,18–20]. Therefore, it is reasonable to propose that the evolution of AlN regions with poor crystalline quality at the AlN/Si interface may have significant influence on the differences between the cross- and in-plane thermal conductivity values of thin film samples.

Based on the work of Cahill [13] and Jacquot et al. [4], amorphous AlN has a lower thermal conductivity than polycrystalline AlN since there is no coherence in the atomic vibration of amorphous AlN. Therefore, our AlN samples can be considered as a two-layered structure with a low thermal conductive amorphous/disordered interfacial layer and a relatively high thermal conductive top polycrystalline AlN layer. By simply assuming that the film is composed of two distinct layers having thermal conductivities of λ_1 and λ_2 for the films with thicknesses of d_1 and d_2, respectively, the relationship between effective thermal conductivity λ_{eff} with the other parameters can be expressed by:

$$\frac{(d_1+d_2)}{\lambda_{eff}}=\frac{d_1}{\lambda_1}+\frac{d_2}{\lambda_2} \tag{6}$$

According to Eq. (6) and the results of the cross-sectional TEM, it is clear that the lower thermal conductivity in the interfacial region causes the significant decrease in the effective thermal conductivity at a film thickness of about 300 nm.

4. Conclusion

This work presents a modified measurement procedure to determine the cross- and in-plane thermal conductivities of the AlN thin films. In this study, the differential 3ω technique was used to analyze the thickness dependency of the cross- and in-plane thermal conductivity of AlN thin films deposited using the magnetron reactive sputtering. The experimental results have shown that both cross- and in-plane thermal conductivities of the AlN thin films are significantly reduced compared to that of their bulk material counterparts. Furthermore, the film thermal conductivity values of both the cross- and in-plane ones increase with the film thickness, but the increase rate decreases gradually with increasing the film thickness for the cross-plane direction case. The XRD, AFM and TEM results indicated that the grain size of sputtered AlN films increases with the increase in film thickness. According to these results, the increased thermal conductivity of the AlN thin films at a large film thickness is primarily due to the increase in the average grain size of the films. Theoretical analysis suggested that the difference of thermal conductivity values contributed by grain boundary scattering cannot fully explain the experimental data. It was considered that the amorphous and disordered interfacial regions at the AlN/Si interfaces, which have a much lower thermal conductivity than the polycrystalline AlN, played another important role in the differences in the thermal conductivity. This argument was supported by the results of the cross-sectional TEM, which demonstrated that the amorphous and disordered layer at the interface obviously influenced the heat transport in the cross-plane direction of the AlN film. The results indicated that improving the interfacial properties will significantly increase the thermal conductivity and promote the applications of AlN thin films in microelectronic devices. Additionally, this work showed that the AlN thin films can be used in microelectronics and MEMS applications to replace conventional dielectric layers such as SiO_2, and a heat-conducting layer owing to their significantly higher cross- and in-plane thermal conductivities. Finally, it should be noted that the difference between the experimental data and theoretical calculation also implies some other mechanisms influencing the thermal conductivity of the investigated AlN thin films, which is worth further investigations.

Acknowledgement

The authors gratefully acknowledge support from the German BMBF for support under grant 03FH027PX2, the UK Engineering and Physical Sciences Research Council (EPSRC) for support under grant EP/P018998/1 and Knowledge Transfer Partnership No KTP010548.

References

[1] J. Zhou, H.F. Pang, L. Garcia-Gancedo, E. Iborra, M. Clement, M. de Miguel-Ramos, H. Jin, J.K. Luo, S. Smith, S.R. Dong, D.M. Wang, Y.Q. Fu, Discrete microfluidics based on aluminum nitride surface acoustic wave devices, Microfluid. Nanofluid. 18 (4) (2015) 537–548.
[2] M. Clement, L. Vergara, J. Sangrador, E. Iborra, A. Sanz-Hervas, SAW characteristics of AlN films sputtered on silicon substrates, Ultrasonics 42 (1–9) (2004) 403–407.
[3] H. Witte, A. Rohrbeck, K.-M. Günther, P. Saengkaew, J. Bläsing, A. Dadgar, A. Krost, Electrical investigations of AlGaN/AlN structures for LEDs on Si(111), Phys. Status Solidi A 208 (7) (2011) 1597–1599.
[4] A. Jacquot, B. Lenoir, A. Dauscher, P. Verardi, F. Craciun, M. Stölzer, M. Gartner, M. Dinescu, Optical and thermal characterization of AlN thin films deposited by pulsed laser deposition, Appl. Surf. Sci. 186 (1–4) (2002) 507–512.
[5] Y. Zhao, C. Zhu, S. Wang, J.Z. Tian, D.J. Yang, C.K. Chen, H. Cheng, P. Hing, Pulsed photothermal reflectance measurement of the thermal conductivity of sputtered aluminum nitride thin films, J. Appl. Phys. 96 (8) (2004) 4563.
[6] G.A. Slack, R.A. Tanzilli, R.O. Pohl, J.W. Vandersande, The intrinsic thermal conductivity of AlN, J. Phys. Chem. Solids 48 (7) (1987) 641–647.
[7] P.K. Kuo, G.W. Auner, Z.L. Wu, Microstructure and thermal conductivity of epitaxial AlN thin films, Thin Solid Films 253 (1–2) (1994) 223–227.
[8] T.S. Pan, Y. Zhang, J. Huang, B. Zeng, D.H. Hong, S.L. Wang, H.Z. Zeng, M. Gao, W. Huang, Y. Lin, Enhanced thermal conductivity of polycrystalline aluminum nitride thin films by optimizing the interface structure, J. Appl. Phys. 112 (4) (2012) 44905.
[9] S.-M. Lee, D.G. Cahill, Heat transport in thin dielectric films, J. Appl. Phys. 81 (6) (1997) 2590.
[10] D.G. Cahill, K. Goodson, A. Majumdar, Thermometry and thermal transport in micro/nanoscale solid-state devices and structures, J. Heat Transf. 124 (2) (2002) 223.
[11] S.R. Choi, D. Kim, S.-H. Choa, S.-H. Lee, J.-K. Kim, Thermal conductivity of AlN and SiC thin films, Int. J. Thermophys. 27 (3) (2006) 896–905.
[12] R. Kato, A. Maesono, R.P. Tye, Thermal conductivity measurement of submicron-thick films deposited on substrates by modified ac calorimetry (laser-heating Ångstrom method), Int. J. Thermophys. 22 (2) (2001) 617–629.
[13] D.G. Cahill, Thermal conductivity measurement from 30 to 750 K: the 3ω method, Rev. Sci. Instrum. 61 (2) (1990) 802.
[14] T. Borca-Tasciuc, A.R. Kumar, G. Chen, Data reduction in 3ω method for thin-film thermal conductivity determination, Rev. Sci. Instrum. 72 (4) (2001) 2139.
[15] Y. Ju, K. Kurabayashi, K. Goodson, Thermal characterization of anisotropic thin dielectric films using harmonic Joule heating, Thin Solid Films 339 (1) (1999) 160–164.
[16] W.L. Liu, T. Borca-Tasciuc, G. Chen, J.L. Liu, K.L. Wang, Anisotropic thermal conductivity of Ge quantum-dot and symmetrically strained Si/Ge superlattices, J. Nanosci. Nanotechnol. 1 (1) (2001) 39–42.
[17] Y. Lee, G.S. Hwang, Mechanism of thermal conductivity suppression in doped silicon studied with nonequilibrium molecular dynamics, Phys. Rev. B 86 (7) (2012).
[18] J.H. Choi, J.Y. Lee, J.H. Kim, Phase evolution in aluminum nitride thin films on Si(100) prepared by radio frequency magnetron sputtering, Thin Solid Films 384 (2) (2001) 166–172.
[19] A. Bourret, A. Barski, J.L. Rouvière, G. Renaud, A. Barbier, Growth of aluminum nitride on (111) silicon: microstructure and interface structure, J. Appl. Phys. 83 (4) (1998) 2003–2009.
[20] G. Radtke, M. Couillard, G.A. Botton, D. Zhu, C.J. Humphreys, Structure and chemistry of the Si(111)/AlN interface, Appl. Phys. Lett. 100 (1) (2012) 11910.